ChemComm

RSC Publishing

COMMUNICATION

View Article Online
View Journal | View Issue

Cite this: *Chem. Commun.*, 2013, **49**, 6858

Received 28th May 2013,
Accepted 10th June 2013

DOI: 10.1039/c3cc44016h

www.rsc.org/chemcomm

Spatially controlled DNA unzipping by microfluidic interface positioning on a molecule perpendicular to a multicomponent flow†

Naresh K. Mani,[abc] Sergii Rudiuk[abc] and Damien Baigl*[abc]

A DNA molecule is rotated under a transversal electric field to be perpendicular to a longitudinal, multicomponent microfluidic flow. Positioning the interface allows us to control DNA unzipping with spatio-temporal resolution. This demonstrates that a microfluidic gradient can be applied at the single molecule level for a dynamic intramolecular stimulation.

Due to the important roles of molecular gradients in biological and synthetic systems, efforts have been devoted to the realization of controlled gradients at the microscale. The development of numerous microfluidic tools[1,2] has enabled the creation and fine control of molecular gradients *via* diffusion-based and/or flow-based approaches.[3] Microfluidics-based gradient devices have been successfully used to modulate or control various biological processes, such as cell migration,[4] stem cell differentiation,[5] axon guidance,[6] and embryonic development.[7] Microfluidic gradients have also been applied at a single cell level. For instance, a seminal demonstration was reported by Takayama *et al.* who succeeded in delivering small molecules into selected domains inside an individual cell by a partial treatment using a laminar multicomponent flow.[8] However, to our knowledge, microfluidic gradients have never been applied to create a controlled perturbation at a single-molecule level. In this communication, we describe the application of an electric field for positioning a single DNA molecule perpendicularly to a longitudinal, multicomponent microfluidic flow in order to control its unzipping, *i.e.* intramolecular denaturation, with spatio-temporal resolution. The application of electric fields to manipulate DNA molecules in nano- or microfluidic channels has been widely used for applications such as DNA stretching,[9,10] separation,[11–15] concentration,[16] mapping[17–19] or polymer physics investigations.[20–25] In contrast to these classical approaches, where DNA molecules are usually stretched in the same direction as that of the microfluidic flow, here we applied the electric field to rotate a single DNA molecule orthogonally to a multicomponent microfluidic laminar flow composed of a buffer phase and a denaturant phase.

Fig. 1A shows our experimental set-up. It consisted of a microfluidic device having two inlets for creating a laminar flow with two components: a DNA buffer solution (upper phase) and a denaturating solution (lower phase). Under our experimental conditions, the Peclet number varied between 50 and 100 (Table S1, ESI†), which ensured a steep profile of the denaturating agent concentration around the interface position. To apply an electric field perpendicular to the flow, two electrodes were inserted into reservoirs situated at both ends of another channel (the vertical channel in Fig. 1A) perpendicular to the main channel. Finally, a single DNA molecule was tethered to a 10 μm diameter pillar, placed at the crossing region.

Our strategy for intra-molecular control of DNA unzipping is shown in Fig. 1B. First, in the absence of an electric field and denaturating phase flow ($Q_D = 0$), a double-stranded DNA molecule (dsDNA) was tethered to the pillar by streptavidin–biotin binding. Then, constant flows of DNA buffer ($Q_B \neq 0$) and denaturing phase ($Q_D \neq 0$) were applied to keep the interface far from the pillar while stretching the DNA molecule along the flow (Fig. 1B, top left). Then, the application of an increasing electric field gradually rotated DNA (Fig. 1B, top middle) up to an angle close to 90° when the electrostatic attraction created by the electric field overcame the longitudinal force created by the flow (Fig. 1B, top right). The electric field was then kept constant and the increase in Q_D allowed us to maintain the interface at different positions, thus inducing partial DNA denaturation, or unzipping, when a steep denaturant concentration gradient was created along the DNA molecule (Fig. 1B, bottom).

The intramolecular unzipping experiment was performed as follows. First, the PDMS surface of the microfluidic channel was covalently covered with streptavidin prior to attaching to a PDMS-coated microscopy glass slide (see ESI,† Materials and

[a] *Department of Chemistry, Ecole Normale Supérieure, 75005 Paris, France. E-mail: damien.baigl@ens.fr; Web: http://www.baigllab.com/; Tel: +33 1 4432 2405*
[b] *Université Pierre et Marie Curie – Paris 6, 75005 Paris, France*
[c] *UMR 8640, CNRS, France*

† Electronic supplementary information (ESI) available: Materials and methods and Table S1. See DOI: 10.1039/c3cc44016h

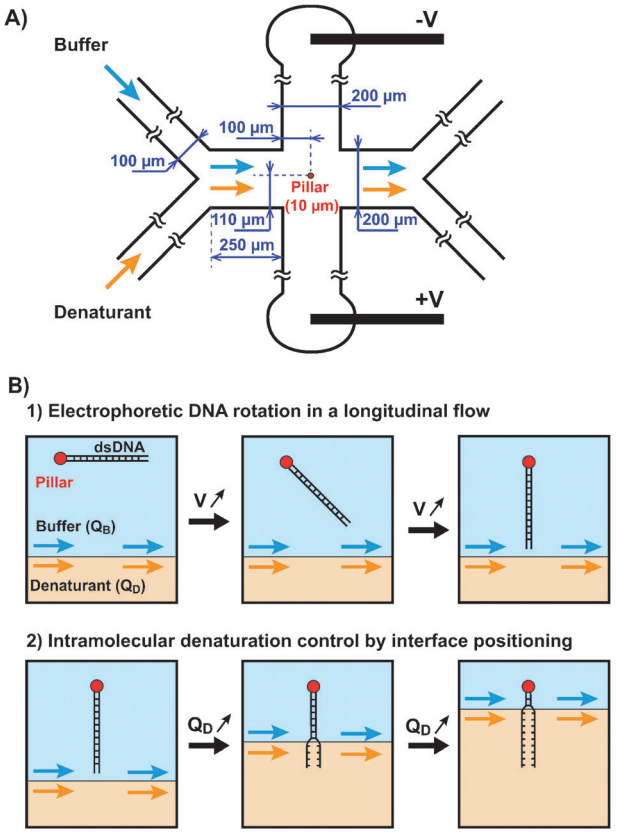

Fig. 1 Experimental set-up and concept. (A) A microfluidic device, made of PDMS, contains two inlets (one for a DNA buffer solution, another one for a denaturant solution), one main channel and two outlets. The main channel is crossed by another channel, along which an electric field is generated from two electrodes. A single pillar (10 µm in diameter) is at the crossing region. All channels are 7.5 µm high. (B) A monobiotinylated double-stranded DNA (dsDNA) is attached to the streptavidinated pillar in the absence of an electric field. The electric field is increased to bring the DNA molecule perpendicular to the flow axis (1). Increasing the denaturant flow rate allows one to maintain the interface at different positions of the molecule, thus unzipping DNA in a spatio-temporally controlled fashion (2).

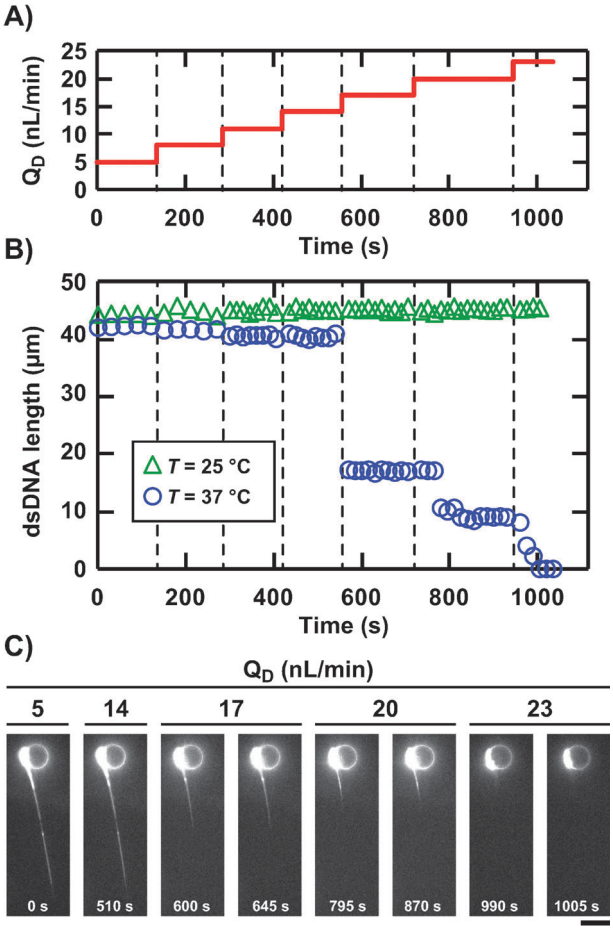

Fig. 2 DNA unzipping by microfluidic interface positioning. (A) Flow rate of the denaturant phase (Q_D) as a function of time. The flow rate of the buffer phase (Q_B = 50 nL min^{-1}) and the electric field (400 V cm^{-1}) are fixed. (B) Length of a dsDNA molecule as a function of time under non-denaturating (T = 25 °C, green triangles) and denaturating (T = 37 °C, blue circles) conditions. (C) Fluorescence microscopy images of the DNA molecule under denaturating conditions as a function of time. The scale bar is 10 µm.

methods for details). The device was then filled with a 0.3 µM solution of monobiotinylated λDNA concatemers (3 copies of λDNA per molecule, *i.e.* 145 500 base pairs, in average) in a buffer composed of 10× Tris-EDTA and YOYO-1 DNA fluorescent dye (60 nM). At this step, the conjugation led to one or several concatemers bound to the pillar and the experiment continued only in the former case. After binding of DNA to the pillar, the flow rate of the DNA buffer solution was fixed at Q_B = 50 nL min^{-1}. Then, the denaturant solution (89% v/v formamide in 10× Tris-EDTA) was added into the microfluidic device at a starting flow rate of Q_D = 5 nL min^{-1}. An electric field of 400 V cm^{-1} was applied to rotate DNA. Under these conditions, DNA could be maintained almost perpendicular to the flow in the whole range of investigated flow rates. Lower electric fields led to smaller angles with respect to the flow direction while much higher fields induced DNA breakage or detachment from the pillar.

We applied a stepwise increase in Q_D (Fig. 2A), and DNA was observed using fluorescence microscopy. Since YOYO-1 is an intercalator that specifically dyes the double-stranded, non-denaturated part of DNA, we characterized the course of local DNA denaturation, or unzipping, by measuring the length of the fluorescent dsDNA part (Fig. 2B and C). A first experiment was performed at 37 °C, a temperature at which DNA is fully denaturated in an 89% v/v formamide solution. Fig. 2 shows that for each denaturant flow rate, dsDNA rapidly reached a stable length that could be maintained as long as the flow rate was not changed. For the lower flow rates, a slight decrease in the time-average dsDNA length was observed (from 42.2 ± 0.2 µm to 40.4 ± 0.4 µm) with an increase in Q_D from 5 nL min^{-1} to 14 nL min^{-1}. In this regime of Q_D, the interface remained too far from DNA to induce significant denaturation. Interestingly, a strong and stepwise decrease in dsDNA length (17.0 ± 0.2 µm and 9.4 ± 0.8 µm) was observed with a further increase in Q_D (17 nL min^{-1} and 20 nL min^{-1}, respectively). Under these conditions, it was thus possible to maintain a single DNA molecule in different partially denaturated states, thanks to the local gradient of formamide along the concatemer. For higher flow rates ($Q_D \geq$ 23 nL min^{-1}), dsDNA could not be distinguished anymore, which was attributed to full

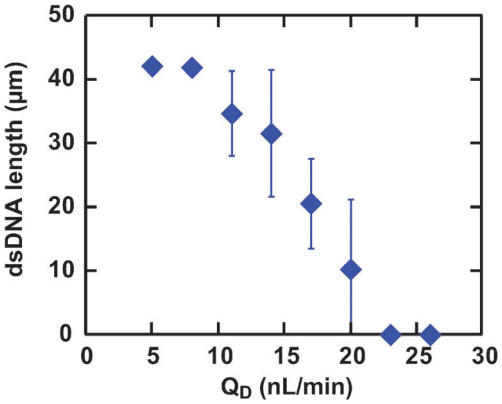

Fig. 3 Length of the dsDNA molecule as a function of the denaturant flow rate (Q_D). The flow rate of the buffer phase (Q_B = 50 nL min^{-1}) and the electric field (400 V cm^{-1}) are fixed. Symbols and error bars show mean values ± SD from triplicates. Error bars are not shown when they are smaller than the symbol size. T = 37 °C.

denaturation by formamide. To ensure that the extinction of YOYO-1 fluorescence was due to local denaturation, we performed a control experiment at 25 °C, a temperature at which DNA is not denaturated in a 89% v/v formamide solution. Fig. 2B (green triangles) shows that the whole concatemer remained fluorescent for the whole range of flow rates. This shows that DNA can be observed in both formamide and buffer solutions but only when it is double-stranded. Therefore, the decrease in dsDNA length observed at 37 °C (denaturating conditions) is unambiguously attributed to the partial DNA unzipping.

We then investigated how DNA unzipping could be spatially controlled by positioning the buffer/denaturant interface. Fig. 3 shows the average dsDNA length as a function of Q_D in triplicate experiments. Although a significant variability between experiments was observed, three features were reproducibly observed. At a low Q_D, the formamide flow was localized far from DNA and no denaturation was observed. Conversely, at a high Q_D, full denaturation was always achieved. Interestingly, in the intermediate range of Q_D values, the dsDNA length significantly decreased with an increase in Q_D due to the successive positions of the buffer/denaturant interface that progressed across the DNA molecule.

We described a microfluidic device in which a single DNA molecule was electrostatically maintained perpendicular to a multicomponent flow composed of a buffer and a denaturing solution. We showed for the first time that a simple control of the flow rates of the solution allowed us to move the buffer/denaturant interface at different positions across the DNA molecule, resulting in successive, stable, partially denaturated states. The spatial resolution of our approach is of the order of a few micrometers. Knowing that 1 μm of fully stretched DNA corresponds to about 3 kbp, which is also the typical size of a gene, our method opens the possibility of intramolecularly stimulating large genomic DNA molecules, with a resolution down to a single gene level, by using a straightforward and robust hydrodynamic principle. Our concept was demonstrated here using a buffer/denaturant interface to control a simple unzipping process. By using other flow compositions, it can be applied to generate various kinds of chemical or biochemical stimulations with unprecedented control at the intramolecular level. For instance, using compaction agents in one phase will enable dynamic intramolecular control of DNA higher-order structure, with immediate applications for synthetic biology and *in vitro* gene regulation. Moreover, the use of more elaborate gradient-generating devices, by improving the position and sharpness of the interface, will allow intramolecular stimulations with improved spatial resolution. Pushing the technology to a single base-pair resolution, for instance, would create new perspectives for DNA mapping and personal genomics.

This work was supported by the European Research Council (ERC) [European Community's Seventh Framework Programme (FP7/2007-2013)/ERC Grant agreement no 258782], the Institut Universitaire de France (IUF), and the Mairie de Paris [Emergence(s) 2012].

Notes and references

1 N. L. Jeon, S. K. W. Dertinger, D. T. Chiu, I. S. Choi, A. D. Stroock and G. M. Whitesides, *Langmuir*, 2000, **16**, 8311–8316.
2 S. K. W. Dertinger, D. T. Chiu, N. L. Jeon and G. M. Whitesides, *Anal. Chem.*, 2001, **73**, 1240–1246.
3 S. Kim, H. J. Kim and N. L. Jeon, *Integr. Biol.*, 2010, **2**, 584–603.
4 N. Li Jeon, H. Baskaran, S. K. W. Dertinger, G. M. Whitesides, L. Van de Water and M. Toner, *Nat. Biotechnol.*, 2002, **20**, 826–830.
5 B. G. Chung, L. A. Flanagan, S. W. Rhee, P. H. Schwartz, A. P. Lee, E. S. Monuki and N. L. Jeon, *Lab Chip*, 2005, **5**, 401–406.
6 S. K. W. Dertinger, X. Jiang, Z. Li, V. N. Murthy and G. M. Whitesides, *Proc. Natl. Acad. Sci. U. S. A.*, 2002, **99**, 12542–12547.
7 E. M. Lucchetta, J. H. Lee, L. A. Fu, N. H. Patel and R. F. Ismagilov, *Nature*, 2005, **434**, 1134–1138.
8 S. Takayama, E. Ostuni, P. LeDuc, K. Naruse, D. E. Ingber and G. M. Whitesides, *Nature*, 2001, **411**, 1016.
9 S. Ferree and H. W. Blanch, *Biophys. J.*, 2003, **85**, 2539–2546.
10 G. C. Randall, K. M. Schultz and P. S. Doyle, *Lab Chip*, 2006, **6**, 516–525.
11 J. Han and H. G. Craighead, *Science*, 2000, **288**, 1026–1029.
12 P. S. Doyle, J. Bibette, A. Bancaud and J.-L. Viovy, *Science*, 2002, **295**, 2237.
13 N. Kaji, Y. Tezuka, Y. Takamura, M. Ueda, T. Nishimoto, H. Nakanishi, Y. Horiike and Y. Baba, *Anal. Chem.*, 2004, **76**, 15–22.
14 N. Nazemifard, S. Bhattacharjee, J. H. Masliyah and D. J. Harrison, *Angew. Chem., Int. Ed.*, 2010, **49**, 3326–3329.
15 T. Yasui, N. Kaji, R. Ogawa, S. Hashioka, M. Tokeshi, Y. Horiike and Y. Baba, *Anal. Chem.*, 2011, **83**, 6635–6640.
16 D. Stein, Z. Deurvorst, F. H. J. van der Heyden, W. J. a. Koopmans, A. Gabel and C. Dekker, *Nano Lett.*, 2010, **10**, 765–772.
17 R. Riehn, M. Lu, Y.-M. Wang, S. F. Lim, E. C. Cox and R. H. Austin, *Proc. Natl. Acad. Sci. U. S. A.*, 2005, **102**, 10012–10016.
18 B. R. Cipriany, R. Zhao, P. J. Murphy, S. L. Levy, C. P. Tan, H. G. Craighead and P. D. Soloway, *Anal. Chem.*, 2010, **82**, 2480–2487.
19 W. Reisner, N. B. Larsen, A. Silahtaroglu, A. Kristensen, N. Tommerup, J. O. Tegenfeldt and H. Flyvbjerg, *Proc. Natl. Acad. Sci. U. S. A.*, 2010, **107**, 13294–13299.
20 J. J. Jones, J. R. C. van der Maarel and P. S. Doyle, *Phys. Rev. Lett.*, 2013, **110**, 068101.
21 J. Wang and C. Lu, *J. Appl. Phys.*, 2007, **102**, 074703.
22 C. Zhang, P. G. Shao, J. a. van Kan and J. R. C. van der Maarel, *Proc. Natl. Acad. Sci. U. S. A.*, 2009, **106**, 16651–16656.
23 C. Zhou, W. W. Reisner, R. J. Staunton, A. Ashan, R. H. Austin and R. Riehn, *Phys. Rev. Lett.*, 2011, **106**, 248103.
24 A. G. Balducci, J. Tang and P. S. Doyle, *Macromolecules*, 2008, **41**, 9914–9918.
25 J.-W. Yeh, A. Taloni, Y.-L. Chen and C.-F. Chou, *Nano Lett.*, 2012, **12**, 1597–1602.

